Eur Biophys J (1996) 25: 105–113

ARTICLE

Andreas Janshoff · Claudia Steinem · Manfred Sieber
Hans-Joachim Galla

Specific binding of peanut agglutinin to G_{M1}-doped solid supported lipid bilayers investigated by shear wave resonator measurements

Received: 22 July 1996 / Accepted: 12 September 1996

Abstract This study deals with the specific interaction between the lectin peanut agglutinin (PNA) from *Arachis hypogaea* and the ganglioside G_{M1} which was incorporated in a solid supported lipid bilayer immobilized on a gold electrode placed on top of an AT-cut quartz crystal. Bilayer formation was reached by self-assembly processes. The first monolayer consists of octanethiol attached to the gold surface via chemisorption and the second monolayer was immobilized by vesicle fusion on the preformed hydrophobic surface. We managed to keep unspecific binding to a minimum by using a phospholipid matrix consisting of 1-palmitoyl-2-oleoyl-*sn*-glycero-3-phosphocholine (POPC). Lectin binding to ganglioside G_{M1} containing membranes was determined by a decrease of the resonant frequency of the quartz crystal. The minimum amount of receptor within the membrane which is necessary to obtain a complete protein monolayer was found to be less than 2 mol%. The adsorption isotherm of PNA to G_{M1} was recorded and analyzed to be of Langmuir type, exhibiting a binding constant of PNA to the ganglioside of $8.3 \cdot 10^5\,M^{-1}$. The good agreement of the calculated Langmuir adsorption isotherm with the obtained experimental data implies that protein multilayers are not formed and that interactions between the adsorbents can be neglected. Furthermore, the association constants of two different saccharides, β-Gal*p*-(1→3)-GalNAc exhibiting a strong binding to PNA in solution, and β-D-galactose with a much lower affinity were estimated by determining the equilibrium concentration of PNA attached to the surface. Moreover we were able to remove the attached lectin monolayer by digestion of the protein with pronase causing an increase in the resonant frequency which almost reversed the frequency shift to lower frequencies during adsorption. An even more complex system was built up by the use of digoxigenin-labeled PNA which also binds to the solid supported membrane containing the receptor G_{M1}. The immobilized lectin was recognized by anti-digoxigenin-F_{ab}-fragments, which is measurable by a further decrease of the resonant frequency. For all binding processes we found larger frequency shifts for a complete protein monolayer than predicted by Sauerbrey's equation, clearly showing that in addition to mass loading viscoelastic changes occur at the lipid-protein interface.

Key words Quartz crystal microbalance (QCM) · Impedance spectroscopy · Solid supported lipid bilayers · Lectins · Gangliosides

Abbreviations DIG digoxigenin · DK dielectric permittivity · LUV large unilamellar vesicle · OT octanethiol · PNA peanut agglutinin · POPC 1-palmitoyl-2-oleoyl-*sn*-glycero-3-phosphocholine · QCM quartz crystal microbalance · β-Gal*p*-(1→3)-GalNAc 2-acetamido-2-deoxy-3-O-D-galactopyranosyl-D-galactopyranose

1 Introduction

Piezoelectric sensors such as the quartz crystal microbalance (QCM) are gaining widespread interest in many fields of analytical chemistry, biotechnology and recently in biochemistry. Bulk shear wave resonators have been used for a long time as a microgravimetric sensor for deposition processes in the gas phase. According to Sauerbrey, mass loading onto a quartz surface causes a proportional shift in the resonant frequency of the shear resonator (Sauerbrey 1959). The development of quartz crystal units operating under liquid loading with one side of the crystal under water has opened up a variety of new applications for shear wave resonators such as monitoring adsorption processes in electrochemistry (Xu and Schlenoff 1959; Schneider and Buttry 1993; Benje et al. 1986) and biomass growth for biotechnological control (Nivens et al. 1993). The development of biosensor devices based on immunoassays (Mu-

A. Janshoff · C. Steinem · M. Sieber · H.-J. Galla (✉)
Institute of Biochemistry, Westfälische Wilhelms-University, Wilhelm-Klemm-Strasse 2, D-48149 Münster, Germany

ramatsu et al. 1987; Koenig and Graetzel 1994) and quantification of ligand receptor interactions (Ebato et al. 1992) became possible. Most of the present studies made use of the so called 'active oscillator method' in which the quartz resonator is part of an oscillator circuit equipped with high gain amplifier units necessary to cope with the increased damping due to the viscous coupling of the liquid. The oscillator method has the advantage of being an inexpensive and very sensitive method to detect small amounts of adsorbed molecules e.g. proteins (Muratsugu et al. 1993) or nucleic acids (Yamagushi and Schimomura 1993). Alternatively, impedance spectroscopy in the frequency range of the resonant frequency of the quartz crystal was performed to obtain more detailed information, especially about the viscoelastic properties of the adsorbed material.

In this paper we used the QCM to study the interaction of the lectin peanut agglutinin (PNA) with the ganglioside G_{M1} embedded in a phospholipid matrix. We chose this interaction because of its importance in many fields of biochemistry. Lectins exhibit a number of interesting properties concerning their carbohydrate binding specificity. Currently, lectins have an important application in typing blood, separating leukocytes from erythrocytes, determining the secretor status, or causing cell agglutination as a prerequisite for plasma preparation. Certain lectins possess the ability to distinguish normal from malignant cells because of their different cell surface antigens, especially the distribution of cell confined glycoproteins. This makes lectins possible candidates for anti-tumor active substances. Since the medical and biochemical importance of lectins is immense, great need exists for characterization of the specific interaction between different carbohydrate structures and the lectins.

The study of ligand receptor interaction at functionalized surfaces often implies difficulties concerning the orientation of the receptor on a well defined surface and to prevent an unspecific binding of the protein to the matrix. We solved these problems by the use of solid supported lipid bilayers prepared according to Steinem et al. (1996). A clean gold surface was initially covered with an alkanethiol via self-assembly in order to form a stable chemisorbed monolayer. The second monolayer consisting of the ganglioside/phospholipid mixture was deposited by fusion of unilamellar vesicles on the preformed hydrophobic monolayer. The formation process was followed by impedance spectroscopy where the gold electrode on the resonator surface serves as the working electrode. With this setup we were able to quantify the binding of PNA to the ganglioside G_{M1}. The lectin PNA from *Arachis hypogaea* (M = 110 000 g/mol) consisting of four identical subunits each possessing a molecular weight of 27 000–28 000 g/mol exhibits a specific binding to the carbohydrate structure β-Gal*p*-(1 → 3)-GalNAc (Goldstein and Hayes 1978). It also shows similar immunological behavior of the anti-T antibody which makes it a useful tool to detect human malignant cells carrying the T-cell antigen on the surface. The QCM allows the detection of the PNA binding to phospholipid layers with various amounts of receptor as well as the inhibitory effect of β-D-galactose and β-Gal*p*-(1 → 3)-GalNAc. Furthermore, the two-dimensional protein layer was used as the basic element for the specific binding of an antibody. In order to prove the suitability for biosensor application, in which regeneration of the sensor surface is very important, we investigated the digestion of the protein monolayer by pronase.

2 Materials and methods

2.1 Materials

1-Palmitoyl-2-oleoyl-*sn*-glycero-3-phosphocholine was purchased from Avanti Polar Lipids (Alabaster, AL, USA). G_{M1}, PNA and the sugars β-Gal*p*-(1 → 3)-GalNAc and β-D-galactose were from Sigma (Deisenhofen, Germany), octanethiol was from Fluka (Neu Ulm, Germany). Pronase, digoxigenin-labeled PNA and the anti-digoxigenin-labeled F_{ab}-fragments were obtained from Boehringer (Mannheim, Germany). Water was first purified by a Millipore water purification system MilliQ RO 10 Plus and finally by the Millipore ultrapure water system MilliQ Plus 185 (18 MΩ/cm). The 5 MHz overtone polished AT-cut quartz crystals (plano-plano) were from KVG (Niederbischofsheim, Germany). The silver conductive adhesive was from the Epoxy-GmbH (Fürth/Odw., Germany) and the silicon glue (Elchsiegel) from Rhône Poulenc (Leverkusen, Germany). The gold (99.999% purity) used for the gold electrodes of the surface of the quartz plates was a generous gift from DEGUSSA (Hanau, Germany), the chromium was purchased from Balzers (Balzers, Liechtenstein).

2.2 Impedance spectroscopy

AC impedance spectroscopy was performed by a continuous wave impedance gain/phase analyzer SI 1260 from Solartron instruments (Great Britain). The magnitude of the impedance $|Z(\nu)|$ as well as the phase angle $\Phi(\nu)$ between current and voltage were recorded in the frequency range of 10^{-1} to 10^{6} Hz with an AC amplitude of 30 mV and 0 mV DC offset. 80 data points were sampled at logarithmic spacing by a personal computer. The electrochemical cell is shown in Fig. 1 and consists of the quartz crystal with one gold electrode serving as the working electrode and a platinized platinum wire as the counter electrode. Quantitative analysis of the spectra was performed by fitting the parameters of the assumed electrical model to the data ($|Z(\nu)|$) by means of a non-linear-least square-fit according to the Levenberg-Marquardt algorithm (Bevington 1969). The equivalent circuit used for the fitting procedure consists of a resistance in series to a capacitance. The resistance represents the ohmic nature of the electrolyte and the capacitance the electrical behavior of the lipid bilayer. The resistance of the bilayer was very high and therefore neglected in the analysis.

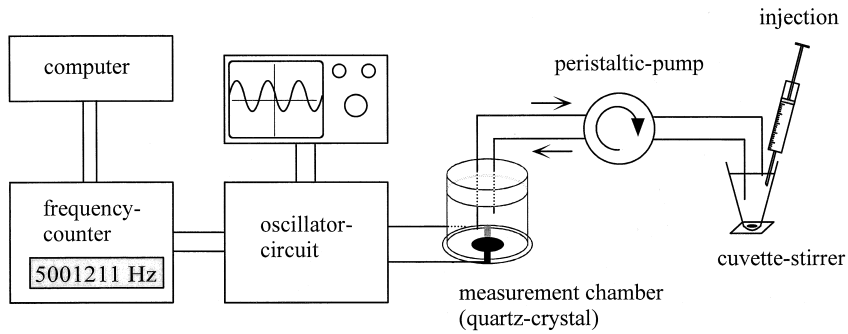

Fig. 1 Schematic diagram of the experimental setup used for the QCM-measurements

2.3 Quartz measurements

The experimental setup for the quartz measurements used in the present study is schematically depicted in Fig. 1. The core component of the system is the quartz resonator. Plano-plano AT-cut quartz resonators with 14 mm diameter and a fundamental resonance frequency of 5 MHz were coated with gold electrodes on both sides as described elsewhere (Steinem et al. 1996). The electrodes were designed as shown in Fig. 1 with an area of 0.33 cm^2. The measuring chamber was formed by a small glass tube fixed on the quartz plate with a silicon glue. The gold electrodes were connected to the oscillator circuit via thin silver wires which are fixed on the gold electrodes by a conductive adhesive. A study of Teuscher et al. revealed that a conductive adhesive improves the stability of the oscillation significantly (Teuscher and Garell 1995). After the quartz dish was mounted into a crystal holder, which fixes only the glued glass tubes in order to avoid any contact with the quartz-crystal, the measuring chamber was closed by a stopper equipped with an inlet and an outlet to connect the chamber with a peristaltic pump. The whole flow system takes a volume of 2 ml. The crystal and the oscillator circuit were placed in a temperature controlled chamber which also serves as a Faraday cage. The temperature was kept at 23 °C. The oscillator circuit consists mainly of an integrated circuit SN74LS124N from Texas instruments connected to a frequency counter from Hewlett Packard (HP 53181A) and an oscilloscope in order to control the oscillation. The data were collected by a personal computer via a serial interface from the frequency counter.

2.3.1 Calibration of the QCM in solution

In order to perform a calibration of the QCM used in this study we applied the method of electrodeposition of copper as described elsewhere (Hillier and Ward 1992). Deposition and frequency detection were performed under liquid loading. Following the theory of Sauerbrey (Sauerbrey 1959) the observed decrease in frequency should be proportional to the change in mass on the quartz resonator.

$$\Delta f = \frac{-2f_0^2 \Delta m}{A\sqrt{\rho_q \mu_q}}, \qquad (1)$$

where f_0 denotes the fundamental resonant frequency, A the electrode area, ρ_q the density of the quartz (ρ_q = 2.648 g/cm^3) and μ_q the shear modulus of the quartz ($\mu_q = 2.947 \cdot 10^{11}$ dyne/cm^2). Equation (1) can be reduced to

$$\Delta f = -C_f \cdot \Delta m, \qquad (2)$$

where C_f denotes the integral mass sensitivity which amounts to 0.11 Hz/ng in our case, corresponding to 0.036 Hz · cm^2/ng. The value is much too low with respect to Sauerbrey's equation (Eq. (1)) (0.057 Hz · cm^2/ng) but is still reasonable considering the scrutiny of Hillier and Ward (1992) who predicted the same value of 5 MHz plano-plano AT-cut quartz resonators plated with copper. They pointed out that plano-plano crystals suffer more energy loss from field fringing at the electrode edge than plano-convex quartz resonators.

2.3.2 Binding assay

Buffer solution was pumped through the measuring cell with a flow rate of 500 µl/min until a stable baseline was reached. The protein solution, dissolved in the same buffer, was added with a Hamilton syringe to a small temperature controlled vessel outside the Faraday cage. The experiments were taken out at 23 °C, except for the vesicle fusion, which was carried out at 40 °C.

2.4 Preparation of lipid bilayers on gold

First, the gold electrode of the quartz was immersed in a self-assembly solution of 1 mM octanethiol in ethanol for 30 min. Afterwards the gold surface was rinsed several times with ethanol in order to remove remaining thiols and then rinsed with a buffer solution consisting of 50 mM Tris, 200 mM NaCl, pH 7.4 to remove the ethanol.

To create the second monolayer of ganglioside containing phospholipids large unilamellar vesicles (LUVs) of 1-palmitoyl-2-oleoyl-*sn*-glycero-3-phosphocholine (POPC) in the same buffer solution with different amounts of the ganglioside G_{M1} were prepared by the extrusion method as described elsewhere (Steinem et al. 1996). The vesicles had diameters of about 100 nm. The lipid bilayer

was formed by adding the preformed vesicles to the hydrophobic monolayer of octanethiol. The preparation was carried out at 40 °C. After one hour the fusion process was finished and the remaining vesicles were removed by rinsing the electrode surface several times with buffer solution. The surface should never be dried during the preparation and the measurement period.

3 Results and discussion

3.1 Characterization of lipid bilayer formation on shear resonators

Impedance spectroscopy has been widely accepted as a powerful tool to determine electrode coverage with ultrathin organic films serving as insulators on the bulk surface (Steinem et al. 1996; Terrettaz et al. 1993; Stelzle et al. 1993; Janshoff et al. 1996). Here, we mainly use this technique to confirm the completeness of the immobilized lipid bilayer. Figure 2 shows typical impedance spectra of a chemisorbed monolayer of octanethiol (OT) and the whole bilayer consisting of a second monolayer of the phospholipid POPC subsequently adsorbed on top of the hydrophobic OT-layer by vesicle fusion. The solid lines represent the fitting results according to the equivalent circuit which is also depicted in Fig. 2. As this simple circuit describes the situation of the immobilized bilayers very well, we leave out more sophisticated models to retain interpretable results. The capacitance of the bilayer $C_{OT/POPC}$ and of each monolayer C_{OT}, C_{POPC} is a sensitive measure of the completeness of the films and is therefore well suited to control the preparation of the bilayers. Typical results for the OT-monolayer exhibit a mean capacitance of (2.2 ± 0.1) $\mu F/cm^2$, the subsequently produced bilayer provides a mean value of (1.0 ± 0.1) $\mu F/cm^2$. Assuming series connection of both capacitances, C_{OT} and C_{POPC} the POPC-monolayer exhibits a mean capacitance of (1.8 ± 0.2) $\mu F/cm^2$. The values for the capacitances are average values obtained from 10 independent measurements. Figure 3 shows the time resolved dependence of the resonant frequency caused by the fusion of LUVs of POPC on a hydrophobic monolayer of OT at 40 °C. The change in frequency amounts to (230 ± 30) Hz obtained from three independent measurements. This frequency shift is considerably higher compared to the expected frequency decrease derived from the Sauerbrey equation (Sauerbrey 1959). Assuming a defined lipid monolayer with a molecular area of 0.4–0.5 nm^2, complete coverage would result in a frequency shift of 9–10 Hz due to a mass change of 82–91 ng. The reason for such a strong deviation cannot be found exclusively in surface roughness or the field fringing effect. Thus, a multilayer formation of 25 lipid-layers on top of the OT-monolayer or adsorbed vesicles loosely bound to the surface ought to be assumed if only mass effects are considered. However, with regard to the results obtained from the impedance analysis (Fig. 2) and those published by others

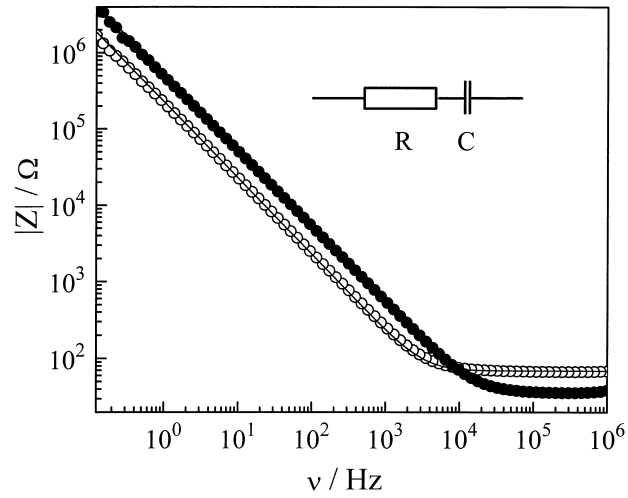

Fig. 2 Impedance spectrum of an octanethiol monolayer (○) chemisorbed on the gold electrode of the quartz plate and after the fusion of POPC-LUVs (●) on the hydrophobic monolayer. The *continuous lines* represent the NLSQ-fits of the assumed network consisting of a capacitance and a resistance in series. Fitting results: $C_{OT} = 2.11$ $\mu F/cm^2$, $R = 69$ Ω; $C_{OT/POPC} = 0.93$ $\mu F/cm^2$, $R = 37$ Ω

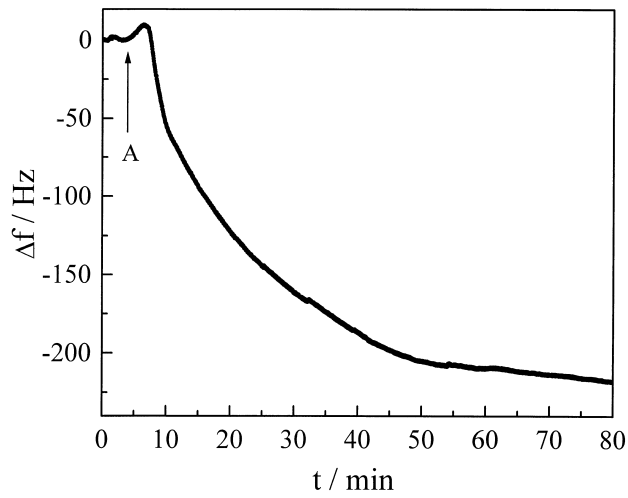

Fig. 3 Frequency shift of the QCM recorded for the injection of POPC-LUVs to an octanethiol monolayer chemisorbed on a gold surface of a quartz plate. *A* indicates the injection of 100 nm POPC-LUVs. The final lipid concentration was 200 μM. The fusion process was carried out at 40 °C

(Kalb et al. 1992) using total internal reflection fluorescence microscopy and fluorescence recovery after photobleaching, a monolayer with high coverage was obtained by the method of vesicle fusion at 40 °C. Kalb et al. reported that multilayer adsorption occurs at lipid concentrations above 1 mM but excess buffer removes the additional layers. Since rinsing the quartz chamber with buffer did not result in any significant frequency shift, it must be assumed that a pure bilayer of OT and POPC was achieved. Therefore the explanation for the very high frequency shifts must be found on the properties of the second mono-

layer itself. Sauerbrey's approach includes several restrictions to keep the theory at a simple level. The linear dependence of the frequency on mass loading is only valid if viscoelastic properties of the adsorbed materials are disregarded. Many publications in the last six years are concerned with the frequency response of a bulk shear wave resonator to several types of viscoelastic loading. Considering the equation derived by Kanazawa and Gordon (1985) in which the decrease of the series resonant frequency is proportional to the square root of the viscosity-density product of the viscous liquid an increasing viscosity at the resonator's surface may be responsible for the large frequency shift. This assumption is supported by the work of Wang et al. (1992) who found an unexpectedly high increase of the resonant frequency of a 5 MHz quartz functionalized with a self-assembled $HS(CH_2)_{15}COOH$-monolayer with increasing pH value. The frequency shift amounts of 1200 Hz in the region of pH 8–9 and was accompanied by a decrease in the motional resistance R from 4500 Ω to 1000 Ω. Though the explanation of this surprising effect is still missing, it must be due to changes of the viscoelasticity, and therefore the structure of the hydrodynamic layer that contains the phospholipid-monolayer and the aqueous solution associated with the thiol-monolayer attached to the gold surface. Considering the drastic change in surface energy due to the adsorption of a hydrophilic monolayer of phospholipids on the hydrophobic surface of the chemisorbed OT-monolayer changes in the hydrodynamic layer could be responsible for the large frequency shift in our case.

Similar to our results, Ohlsson et al. obtained high frequency changes caused by the fusion of vesicles on a hydrophobic surface using a slightly different technique – the detergent depletion technique – to prepare the vesicles (Ohlsson et al. 1995). The main difference between Ohlsson's and our result exists in the saturation of the frequency shift. In our experiments the frequency decrease saturates after one hour whereas Ohlsson et al. could not detect a saturation of the frequency decrease. This fact could be an indication for the formation of multilayers by the use of detergents during the vesicle formation. In summary, one must say that it remains to be elucidated which are the reasons for the unexpected high frequency shifts accompanied by changes of the surface structure.

Another interesting point which remains to be explained is the small increase of the reasonant frequency directly after addition of the vesicle suspension (Fig. 3). This fact could be an indication of a two step process. An increase of the resonant frequency of an oscillator operating in series mode is due to an increase of the motional resistance R when considering the equivalent circuit of a loaded quartz crystal as given in excellent studies by Martin et al. and Kipling and Thompson (Martin et al. 1991; Kipling and Thompson 1990). Contrary to this phenomenon an increasing inductance L causes a decrease in resonant frequency, an effect which obviously dominates the process after several minutes. Network analysis will be necessary to clear up the process in detail.

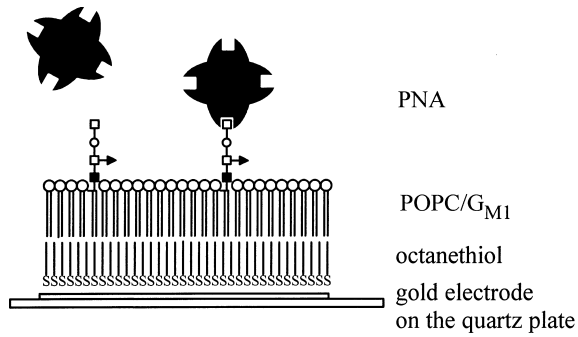

Fig. 4 Schematic view of the solid supported lipid bilayer doped with the receptor lipid on the surface of a gold electrode at the quartz crystal

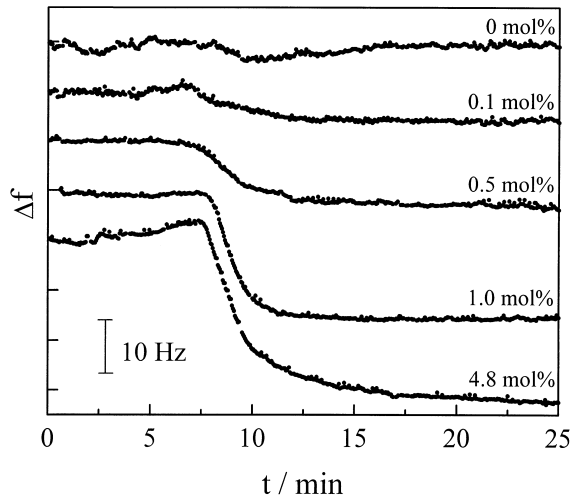

Fig. 5 Time course of the frequency shift of the QCM recorded for the injection of PNA to a POPC monolayer containing different amounts of the receptor lipid G_{M1}. The final protein concentration was 2 μM. The protein solution was added after 7 min

3.2 Adsorption of PNA on G_{M1} doped lipid bilayers

The solid supported lipid bilayer was used to investigate the binding properties of PNA to the ganglioside G_{M1}. Figure 4 depicts schematically the solid supported membrane on the quartz plate doped with the receptor lipid. The specific binding of the protein was determined by the QCM. PNA was added to the vessel after a constant baseline was reached, which was typically after an equilibration of 30 min. The solution with a concentration of 2 μM protein was pumped through the measuring chamber with a flow rate of 500 μl/min. As shown in Fig. 5, the quartz crystal microbalance responded with typical frequency shifts of 6 to 30 Hz by addition of PNA to the immobilized POPC monolayer containing different amounts of the receptor lipid G_{M1}. The adsorption of the lectin shows typical saturation kinetics. No unspecific adsorption took place on pure POPC-monolayers. This is very important with re-

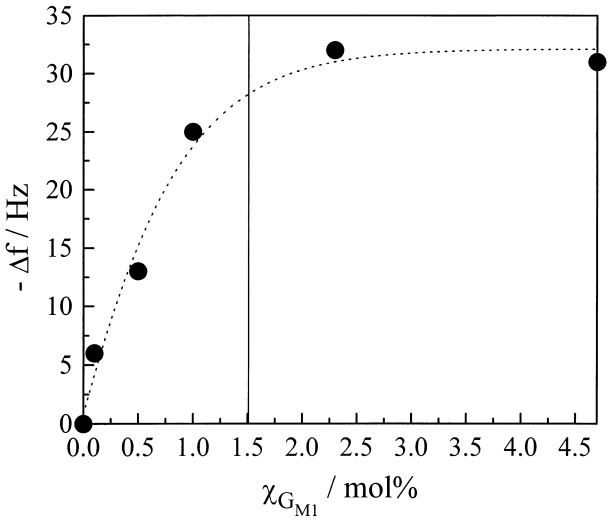

Fig. 6 Dependence of the frequency shift on the G_{M1} content in the POPC monolayer. The values for Δf were obtained from the decrease in frequency from Fig. 5. The *solid line* indicates the minimal value that is necessary for a complete coverage of PNA on the surface. For further details see text

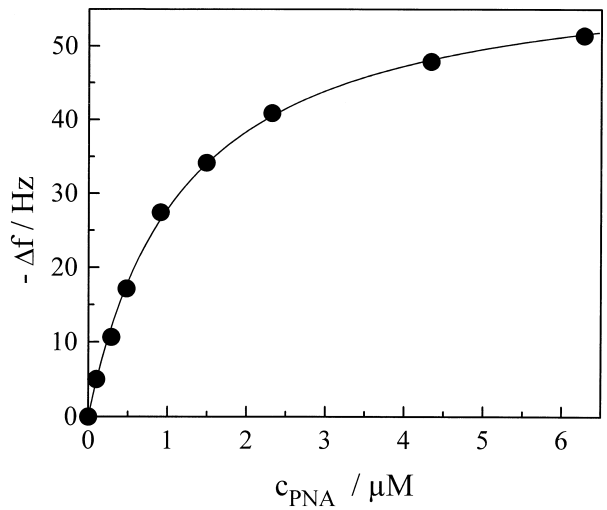

Fig. 7 Dependence of the frequency shift on the PNA concentration in the bulk phase. A monolayer of POPC doped with 4.8 mol% G_{M1} was used to study the binding behavior of PNA to the ganglioside. The high G_{M1} content guaranteed that a complete monolayer of PNA can be reached on the surface. The *continuous line* represents the fit according to the Langmuir adsorption isotherm. The experiment was performed three times and showed high reproducibility

gard to biosensor application and emphasizes the findings that solid supported lipid bilayers with their almost natural lipid environment are well suited for ligand-receptor studies (Stelzle et al. 1993). As expected, phospholipids suppress unspecific interaction very effectively. The frequency shifts increase with increasing amounts of G_{M1} and become constant in the range of 2 mol% G_{M1} (Fig. 6). Assuming an average area per molecule for POPC of 0.5 nm^2, for G_{M1} of 0.7 nm^2 and for PNA of 32 nm^2 (Mehlhorn et al. 1986) the theoretical value of the minimal amount of the receptor lipid G_{M1}, which is necessary to get a complete monolayer of PNA can be estimated to 1.5 mol% G_{M1}. The calculation implies the homogeneous distribution of the ganglioside within the membrane. This seems to be reasonable as this is in good agreement with the experimental data.

Figure 7 depicts the dependence of the frequency shift on the PNA concentration in the bulk phase. In this experiment a POPC monolayer with a content of 4.8 mol% G_{M1} was used in order to guarantee a complete coverage of the surface with PNA. When the concentration of PNA was increased in the bulk phase, the frequency shift shows a typical saturation. Assuming a homogeneous distribution of the receptor lipid in the membrane and independent and equal adsorption sites, the Langmuir adsorption isotherm is a useful model to describe the experimental data. The adsorption equilibrium is

(I) $\quad PNA + G_{M1} \rightleftharpoons PNA\text{-}G_{M1}.$

The relation between the frequency shift and the PNA concentration is given by Eq. (3) since the decrease in frequency is assumed to be proportional to the adsorbed mass of the protein.

$$\Delta f = \Delta f_{max} \cdot \frac{K_a \cdot c_{PNA}}{1 + K_a \cdot c_{PNA}}. \qquad (3)$$

Δf_{max} is the frequency shift upon saturation and K_a is the association constant of PNA and G_{M1}. The assumption that the frequency response is proportional to the amount of adsorbed protein should be reasonable with regard to Sauerbrey's approach (Eq. (1)), which predicts a proportionality between the adsorbed mass and the change in frequency (Sauerbrey 1959). Fitting the parameters to the data of Fig. 7 we obtained a value of $\Delta f_{max} = (61 \pm 1)$ Hz and $K_a = (0.83 \pm 0.04) \cdot 10^6\ M^{-1}$. The fit is in excellent agreement with the theory, which supports the assumption that a defined protein-monolayer is adsorbed. The formation of multilayers can be excluded.

This point leads us to the important question of why the obtained frequency changes are larger than those predicted from Sauerbrey's equation. An expected frequency decrease of 21 Hz for a complete protein monolayer compares with a maximal decrease of 61 Hz obtained by fitting the adsorption isotherm with Eq. (3). Unspecific adsorption at the quartz surface beyond the evaporated gold electrodes was excluded by the measurements shown in Fig. 5, where no significant changes in resonant frequency occur if pure POPC-layers were used. Moreover, the increased roughness of the surface due to the vesicle fusion is probably not the only reason for an enhanced frequency response. The basic element to determine the mass of protein adsorbed on the membrane by use of the frequency shift is based on the fact that proteins behave like rigid films in solution. Adsorbed proteins possess a considerable amount of bound water which also contributes to the frequency response as well as their viscoelastic properties

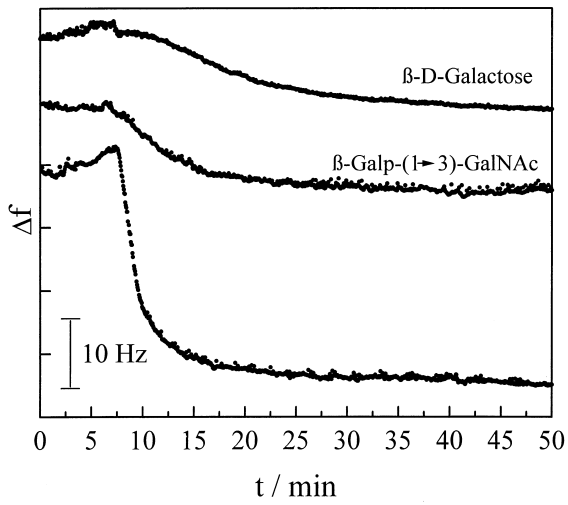

Fig. 8 Time course of the frequency shift recorded after the injection of PNA at a concentration of 2 μM in the presence of 0.265 mM *β*-Gal*p*-(1→3)-GalNAc, 26.5 mM *β*-D-galactose and without inhibitors

which were often omitted. Thus, the viscoelastic behavior of the adsorbed protein layer including the immobilized water and the mass load contribute to the frequency change. This observation was supported by experiments performed in other laboratories. Ohlsson et al. (1995) found that choleratoxin exhibits an unexpected high frequency decrease of about 100 Hz when bound to G_{M1} embedded in a phospholipid matrix. Muratsugu et al. (1993) demonstrated that adsorption of HSA and anti-HSA creates a $|\Delta f/\Delta m|$ relation much larger than predicted from Sauerbrey's equation. The frequency shift depends on the properties of the protein itself what makes a prediction of the amount of adsorbed protein difficult.

3.3 Determination of the association constants of *β*-D-galactose and *β*-Gal*p*-(1→3)-GalNAc

It is known that strong inhibition of hemagglutination, which is induced by PNA occurs if *β*-Gal*p*-(1→3)-GalNAc is added to the agglutination test. The disaccharide binds specifically to PNA. In order to prove the suitability of our setup to quantify the binding constants of different saccharides to PNA in solution we investigated the PNA binding on G_{M1} doped POPC layers in the presence of *β*-Gal*p*-(1→3)-GalNAc and *β*-D-galactose, respectively. Figure 8 shows the time courses of the resonance frequency shifts after addition of 2 μM PNA to G_{M1} containing POPC-monolayers in the presence of 26.5 mM *β*-D-galactose and 0.265 mM *β*-Gal*p*-(1→3)-GalNAc, respectively. For comparison the time course of the frequency change in the absence of an inhibitor is also shown. The binding of PNA in the presence of the corresponding ligand causes a lower frequency decrease than in the absence of ligands owing to a reduced concentration of accessible PNA binding sites in the bulk solution. In order to obtain the intrinsic binding constant $K_{S,i}$ of one binding site of PNA to the corresponding carbohydrate in solution we pursued the following approach. In contrast to the Langmuir adsorption isotherm obtained from PNA in the absence of ligands the situation in the presence of ligands is more complex. Since PNA possesses four identical subunits each capable of binding a ligand with the same intrinsic binding constant $K_{S,i}$ five different PNA-carbohydrate complexes have to be distinguished: PNA, PNA-S, PNA-S_2, PNA-S_3 and PNA-S_4. Except for PNA-S_4 all species are able to bind to the immobilized ganglioside. The corresponding equilibrium at the surface according to Langmuir reads as follows:

$$\text{(II)} \qquad \begin{aligned} 4 \cdot k_{a,i} \cdot c_{PNA} \cdot (1-\theta_g) &= k_{d,i} \cdot \theta_{PNA} \\ 3 \cdot k_{a,i} \cdot c_{PNA\text{-}S} \cdot (1-\theta_g) &= k_{d,i} \cdot \theta_{PNA\text{-}S} \\ 2 \cdot k_{a,i} \cdot c_{PNA\text{-}S_2} \cdot (1-\theta_g) &= k_{d,i} \cdot \theta_{PNA\text{-}S_2} \\ k_{a,i} \cdot c_{PNA\text{-}S_3} \cdot (1-\theta_g) &= k_{d,i} \cdot \theta_{PNA\text{-}S_3} \end{aligned}$$

where θ_g is the total coverage of the surface and can be expressed as the sum of the coverage of each PNA species:

$$\theta_g = \theta_{PNA} + \theta_{PNA\text{-}S} + \theta_{PNA\text{-}S_2} + \theta_{PNA\text{-}S_3}.$$

$k_{a,i}$ and $k_{d,i}$ denote the intrinsic adsorption and desorption rate constants of one binding site at the surface, respectively. After some algebra the Langmuir equation reads:

$$\frac{\Delta f}{\Delta f_{max}} = \frac{K_{a,i} \cdot (4 \cdot c_{PNA} + 3 \cdot c_{PNA-S} + 2 \cdot c_{PNA-S_2} + c_{PNA-S_3})}{1 + K_{a,i} \cdot (4 \cdot c_{PNA} + 3 \cdot c_{PNA-S} + 2 \cdot c_{PNA-S_2} + c_{PNA-S_3})}. \quad (4)$$

The intrinsic Langmuir adsorption constant $K_{a,i} = k_{a,i}/k_{d,i}$ can be derived from the Langmuir adsorption constant K_a (see Eq. (3)) as $K_a = 4 \cdot K_{a,i}$ assuming that all binding sites of the PNA-carbohydrate complexes have the same binding constant to G_{M1}. The sum of the four concentrations in brackets in Eq. (4) represents the total concentration of binding sites $c_{protomer}$ able to interact with the surface confined receptor:

$$c_{protomer} = 4 \cdot c_{PNA} + 3 \cdot c_{PNA\text{-}S} + 2 \cdot c_{PNA\text{-}S_2} + c_{PNA\text{-}S_3}, \quad (5)$$

Considering this protomer concentration in solution, equilibrium between the carbohydrate and PNA-binding sites reads:

$$\text{(III)} \qquad \text{protomer} + S \rightleftharpoons \text{protomer-}S$$

where S denotes the corresponding saccharide. The intrinsic binding constant $K_{s,i}$ can be derived from equilibrium:

$$K_{S,i} = \frac{c_{protomer-S}}{c_{protomer} \cdot c_s} = \frac{c_{protomer-S}}{c_{protomer} \cdot (c_{S,0} - c_{protomer-S})}, \quad (6)$$

where $c_{S,0}$ denotes the initial concentration of the corresponding saccharide added to the measuring cell. $c_{protomer-S}$, c_S and $c_{protomer}$ represent the equilibrium concentrations of the corresponding species. Neglecting the amount of protomer bound to the surface compared with the total amount of protomer ($4 \cdot c_{PNA,0}$) the intrinsic binding constant $K_{S,i}$ can be calculated from the equilibrium concentration of the unbound protomer, $c_{protomer}$:

$$K_{S,i} = \frac{4 \cdot c_{PNA,0} - c_{protomer}}{c_{protomer} \cdot [c_{S,0} - (4 \cdot c_{PNA,0} - c_{protomer})]}. \quad (7)$$

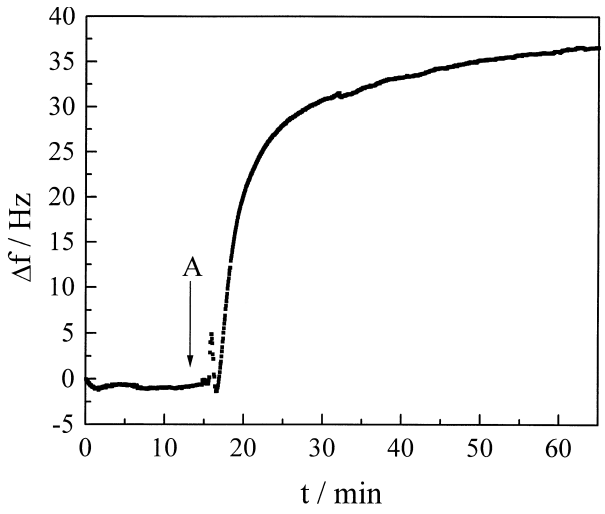

Fig. 9 Response of the frequency on the addition of 0.2% pronase A to a PNA monolayer absorbed on POPC doped with 4.8 mol% G_{M1}

$c_{protomer}$ can be calculated directly from the measured frequency shift Δf (Eq. (4)). In the presence of $c_{S,0} = 0.265$ mM β-Gal*p*-(1→3)-GalNAc the frequency decreases by (13 ± 2) Hz after the addition of $c_{PNA,0} = 2$ μM PNA so that $K_{S,i}$ can be estimated to be (20 000 ± 5000) M^{-1}. The frequency shift that results from the adsorption of 2 μM PNA in the presence of 26.5 mM β-D-galactose amounts to (11 ± 2) Hz which corresponds to a $K_{S,i}$ of (250 ± 50) M^{-1}. Swamy et al. (1991) reported similar binding constants for β-Gal*p*-(1→3)-GalNAc and β-D-galactose using the method of fluorescence titration with the fluorescently labeled 2-(N-dansylamino)2-deoxy-D-β-D-galactose at 15 °C. Caron et al. (1982) as well as Neurohr et al. (1982) studied the binding of β-D-galactose and β-Gal*p*-(1→3)-GalNAc to PNA, respectively, by UV difference spectroscopy at different temperatures and obtained association constants in the same range (Table 1). The comparable results clearly indicate the suitability of QCM to determine binding constants of ligand receptor pairs in solution.

3.4 Digestion of the PNA-monolayer by pronase

With respect to the suitability of the ligand receptor system on solid supported lipid bilayers in biosensor application a reusable sensor surface would be of great advantage. The regain of the receptor molecules G_{M1} embedded in the phospholipid bilayer requires that the protein can be removed from the surface without destruction of the lipid layer. We tried to remove the adsorbed PNA by digestion of the monolayer by pronase. Pronase is an unspecific proteolytic enzyme capable of removing the protein layer without any digestion of the lipid layer. The addition of the enzyme at a concentration of 0.2% to the measuring cell led to an increase of the frequency up to (35 ± 3) Hz after one hour (Fig. 9). Obviously the time course of the resonance frequency exhibits a two step kinetic where a fast increase is followed by a second much slower process. The PNA-monolayer obtained from the specific interaction of a 2 μM protein solution with the POPC monolayer containing 4.8 mol% G_{M1} exhibited a mean frequency decrease of (32 ± 2) Hz (see Fig. 5). Starting from this PNA-monolayer a frequency shift of 35 Hz corresponds to an almost complete digestion of the protein monolayer.

We recorded an impedance spectrum after the digestion-process in order to prove the completeness of the bilayer. The capacitance of the bilayer increases only from 1.0 μF/cm² to 1.05 μF/cm² after protein digestion. The increase in capacitance indicates that only a small amount of the lipid bilayer was removed by the protease treatment. The errors are standard deviations of three independent measurements indicating the high reproducibility of the digestion process.

3.5 Specific binding of anti-digoxigenin-F_{ab}-fragments to a digoxigenin-labeled PNA-monolayer

In this experiment digoxigenin (DIG)-labeled PNA was used instead of PNA in order to create a hapten presenting surface now consisting of proteins. DIG is a steroid and occurs naturally in digitalis plants such as *Digitalis purpurea*. The anti-digoxigenin antibodies against the hapten have been produced in sheep and possess a covalently linked alkaline phosphatase. This assay is mainly used for Western-blotting or for non-radioactive detection of DNA. The antibody-antigen-conjugate is then visualized by a color reaction catalyzed by the alkaline phosphatase. We used this system to enhance the frequency decrease because of the higher molecular weight of the antibody-phosphatase complex than the antibody alone.

Figure 10 shows the typical time course of the series resonance frequency after addition of DIG-labeled PNA

Table 1 Determination of the binding constants $K_{S,i}$ of β-D-galactose and β-Gal*p*-(1→3)-GalNAc to PNA by QCM for T = 23 °C. The errors are the standard deviations of three independent measurements. The reference values for $K_{S,i}$ were taken from [a] Swamy et al. (1991); [b] Caron et al. (1982); [c] Neurohr et al. (1982)

Ligand	$c_{S,0}$/mM	Δf/Hz	$K_{S,i}/M^{-1}$	$K_{S,i}/M^{-1}$ (ref.)
No ligand	–	34 ± 2	–	–
β-D-galactose	26.5	11 ± 2	250 ± 50	690 (15 °C)[a] 1200 (10 °C)[b]
β-Gal*p*-(1→3)-GalNAc	0.265	13 ± 2	20 000 ± 5 000	33 000 (23 °C)[c] 49 000 (15 °C)[a]

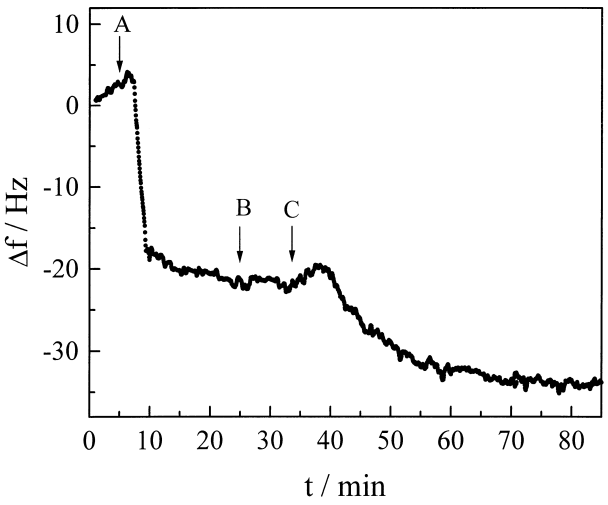

Fig. 10 Frequency response of the QCM on the addition of *A* 2 μM digoxigenin labeled PNA to a POPC monolayer doped with 1 mol% G_{M1}. *B* indicates the exchange of incubation solution by PNA free buffer and *C* anti-digoxigenin-labeled F_{ab} fragments labeled with alkaline phosphatase in a concentration of 90 μg/ml (18 U/ml)

with a concentration of 2 μM (arrow A) to a POPC monolayer doped with 1 mol% G_{M1}. The frequency shift of 26 Hz is comparable to the frequency shift of PNA which is not labeled. When the adsorption of DIG-labeled PNA was finished, the solution was exchanged against pure buffer (arrow B). After a stable baseline was reached anti-DIG-F_{ab}-fragments were added to a final concentration of 18 U/ml (arrow C). A frequency shift of $\Delta f = 15$ Hz was obtained owing to the specific binding of the F_{ab}-fragments to the hapten exposed by the DIG-labeled PNA monolayer. The experiments show that the hapten is exposed to solution and accessible for the antibody.

Acknowledgements This work has been financially supported by the Bundesministerium für Bildung und Forschung (BMBF). We would like to thank W. Wilting from the Institute of Geophysics of the WWU Münster for his extraordinary help in the electronic design of the oscillator circuit. The generous support of the DEGUSSA-AG (Frankfurt/Main, FRG) with gold is gratefully acknowledged.

References

Benje M, Eiermann M, Pittermann U, Weil KG (1986) An improved quartz microbalance. Application to the electrocrystallization and -dissolution of nickel. Ber Bunsenges Phys Chem 90:435–439

Bevington PR (1969) Data reduction and error analysis for the physical science. MacGraw-Hill Book Company, New York

Caron M, Ohanessian J, Becquart J, Gillier-Pandraud H (1982) Ultraviolet difference spectroscopy study of peanut lectin binding to mono- and disaccharides. Biochim Biophys Acta 717:432–438

Ebato H, Herron JN, Müller W, Okahata Y, Ringsdorf H, Suci P (1992) Specific binding of a functional protein layer to a fixed streptavidin matrix: studies with a quartz microbalance. Angew Chem Int Ed Engl 31:1087–1090

Goldstein IJ, Hayes CE (1978) The lectins: carbohydrate-binding proteins of plants and animals. Adv Carbohyd Chem Biochem 35:127–340

Hillier AC, Ward MD (1992) Scanning electrochemical mass sensitivity mapping of the quartz crystal microbalance in liquid media. Anal Chem 64:2539–2554

Janshoff A, Wegener J, Steinem C, Sieber M, Galla H-J (1996) Applications of impedance spectroscopy in biochemistry and biophysics. Acta Biochim Pol 43:339–348

Kalb E, Frey S, Tamm LK (1992) Formation of supported planar bilayers by fusion of vesicles to supported phospholipid monolayers. Biochim Biophys Acta 1103:307–316

Kanazawa KK, Gordon JG (1985) Frequency of a quartz microbalance in contact with liquid. Anal Chem 57:1770–1771

Kipling AL, Thompson M (1990) Network analysis method applied to liquid-phase acoustic wave sensors. Anal Chem 62:1514–1519

Koenig B, Graetzel M (1994) A novel immunosensor for Herpes viruses. Anal Chem 66:341–344

Martin SJ, Edwards Granstaff V, Frye GC (1991) Characterization of a quartz crystal microbalance with simultaneous mass and liquid loading. Anal Chem 63:2272–2281

Mehlhorn IE, Parraga G, Barber KR, Grant CWM (1986) Visualization of domains in rigid ganglioside/phosphatidylcholine bilayers: Ca^{2+} effects. Biochim Biophys Acta 863:139–155

Muramatsu H, Dicks JM, Tamiya E, Karube I (1987) Piezoelectric crystal biosensor modified with protein A for determination of immunoglobulins. Anal Chem 59:2760–2763

Muratsugu M, Ohta F, Miya Y, Hosokawa T, Kurosawa S, Kamo N, Ikeda H (1993) Quartz crystal microbalance for the detection of microgram quantities of human serum albumin: Relationship between the frequency change and the mass of protein adsorbed. Anal Chem 65:2933–2937

Neurohr KJ, Bundle DR, Young NM, Mantsch HH (1982) Binding of disaccharides by peanut agglutinin as studied by ultraviolet difference spectroscopy. Eur J Biochem 123:305–310

Nivens DE, Chambers JQ, Anderson TR, White DC (1993) Long-term on-line monitoring of microbial biofilms using a quartz crystal microbalance. Anal Chem 65:65–69

Ohlsson P-A, Tjaernhage T, Herbai E, Laefas S, Puu G (1995) Liposome and proteoliposome fusion onto solid substrates studies using atomic force microscopy quartz crystal microbalance and surface plasmon resonance. Biological activities of incorporated components. Bioelectrochem Bioenerg 38:137–148

Sauerbrey G (1959) Verwendung von Schwingquarzen zur Wägung dünner Schichten und zur Mikrowägung. Z Phys Chem 155:206–222

Schneider TW, Buttry DA (1993) Electrochemical quartz crystal microbalance studies of adsorption and desorption of self assembled monolayers of alkyl thiols on gold. J Am Chem Soc 115:12391–12397

Swamy MJ, Gupta D, Mahanta SK, Surolia A (1991) Further characterization of the saccharide specifity of peanut (*Arachis hypogaea*) agglutinin. Carbohydr Res 213:59–67

Steinem C, Janshoff A, Ulrich W-P, Sieber M, Galla H-J (1996) Impedance analysis of supported lipid bilayer membranes: A scrutiny of different preparation techniques. Biochim Biophys Acta 1279:169–180

Stelzle M, Weissmüller G, Sackmann E (1993) On the application of supported bilayers as receptive layers for biosensor with electrical detection. J Phys Chem 97:2974–2981

Terrettaz S, Stora T, Duschl C, Vogel H (1993) Protein binding to supported lipid membranes: Investigation of the cholera toxin-ganglioside interaction by simultaneous impedance spectroscopy and surface plasmon resonance. Langmuir 9:136–1369

Teuscher JH, Garell RL (1995) Stabilization of quartz crystal oscillators by a conductive adhesive. Anal Chem 67:3372–3375

Wang J, Frostman LM, Ward MD (1992) Self-assembled thiol monolayers with carboxylic acid functionality: Measuring pH dependent-phase transitions with the quartz crystal microbalance. J Phys Chem 96:5224–5228

Xu H, Schlenoff JB (1995) Kinetics isotherms and competition in polymer adsorption using the quartz crystal microbalance. Langmuir 10:241–245

Yamagushi S, Shimomura T (1993) Adsorption immobilization and hybridization of DNA studied by the use of quartz crystal oscillators. Anal Chem 65:1925–1927